# Combining linear interpolation with extrapolation methods in range-separated ensemble density functional theory

Bruno Senjean, Erik D. Hedegård, Md. Mehboob Alam, Stefan Knecht & Emmanuel Fromager

Taylor & Francis
Taylor & Francis Group
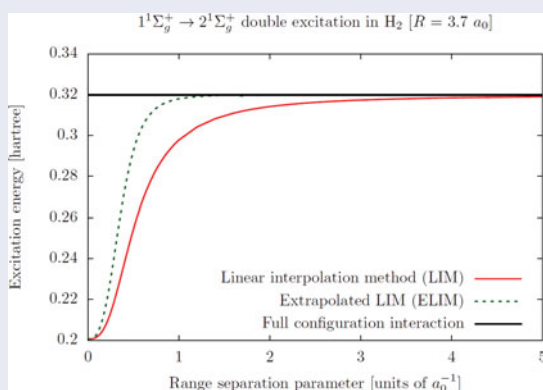
SPECIAL ISSUE IN HONOUR OF ANDREAS SAVIN

# Combining linear interpolation with extrapolation methods in range-separated ensemble density functional theory

Bruno Senjean[a], Erik D. Hedegård[b], Md. Mehboob Alam[a], Stefan Knecht[b] and Emmanuel Fromager[a]

[a]Laboratoire de Chimie Quantique, Institut de Chimie, CNRS/Université de Strasbourg, Strasbourg, France; [b]Laboratory of Physical Chemistry, ETH Zürich, Zürich, Switzerland

## ABSTRACT

The combination of a recently proposed linear interpolation method (LIM), which enables the calculation of weight-independent excitation energies in range-separated ensemble density functional approximations, with the extrapolation scheme of Savin is presented in this work. It is shown that LIM excitation energies vary quadratically with the inverse of the range-separation parameter $\mu$ when the latter is large. As a result, the extrapolation scheme, which is usually applied to long-range interacting energies, can be adapted straightforwardly to LIM. This extrapolated LIM (ELIM) has been tested on a small test set consisting of He, Be, $H_2$ and $HeH^+$. Relatively accurate results have been obtained for the first singlet excitation energies with the typical $\mu = 0.4$ value. The improvement of LIM after extrapolation is remarkable, in particular for the doubly excited $2^1\Sigma_g^+$ state in the stretched $H_2$ molecule. Three-state ensemble calculations in $H_2$ also show that ELIM does not necessarily improves relative excitation energies, even though individual excitation energies are more accurate after extrapolation. Finally, an alternative decomposition of the short-range ensemble exchange–correlation energy is proposed in order to correct for ghost-interaction errors in multi-determinant range-separated ensemble density functional theory calculations. The implementation and calibration of such a scheme are currently in progress.

$1^1\Sigma_g^+ \rightarrow 2^1\Sigma_g^+$ double excitation in $H_2$ [$R = 3.7\ a_0$]

Linear interpolation method (LIM)
Extrapolated LIM (ELIM)
Full configuration interaction

## 1. Introduction

Nowadays, excitation energies are mostly computed by means of time-dependent density functional theory (TD-DFT) [1,2], essentially because of its low computational cost and its relatively good accuracy. Despite this success, standard TD-DFT fails in describing multiple excitations [3] and, in general, multi-configurational effects [4]. Ensemble DFT [5–8] is an alternative to TD-DFT which can, in principle, provide exact excitation energies in a time-independent framework. Despite the fact that developing exchange–correlation functionals for ensembles is

challenging [9–12], thus explaining why ensemble DFT is not yet standard, the use of ensembles in DFT for excited states has reappeared recently in the literature (see, for example, [13–19]). One interesting feature of ensemble DFT is that it offers, when combined with range separation [20], a rigorous framework for developing state-averaged multi-determinant DFT methods [13,21,22].

In practical range-separated ensemble DFT calculations, ground-state functionals are used, simply because short-range ensemble exchange–correlation density functional approximations have not been developed

so far. This leads to curved range-separated ensemble energies [22] and, consequently, to ensemble-weight-dependent excitation energies. Some of the authors recently proposed a linear interpolation method (LIM) [22] which, by construction, provides linear ensemble energies and, therefore, well-defined approximate excitation energies. Promising results have been obtained with LIM, especially for the $2^1\Sigma^+$ charge-transfer state in the stretched $HeH^+$ molecule and the doubly excited $2^1\Sigma_g^+$ state in the stretched $H_2$ molecule. However, in the latter case, the excitation energy was still significantly underestimated [22].

In this work, we propose to adapt the extrapolation scheme of Savin [23–25] to ensembles. The basic idea is to expand the approximate LIM ensemble energy in $1/\mu$, where $\mu$ is the parameter that controls the range separation, and to use this expansion for improving the convergence towards the exact result (i.e. the $\mu \to +\infty$ limit). The paper is organised as follows. After a brief introduction to ground-state range-separated DFT in Section 2.1, ensemble DFT is presented in Section 2.2 and its range-separated extension is discussed in Section 2.3. LIM is then introduced in Section 2.4 and its combination with Savin's extrapolation technique is presented in Section 2.5. After a summary in Section 3 and the computational details in Section 4, results obtained for He, Be, $H_2$ and $HeH^+$ are discussed in Section 5. As a perspective, a correction scheme for ghost-interaction errors in multi-determinant range-separated ensemble DFT is proposed in Section 6. Finally, conclusions are given in Section 7.

## 2. Theory

### 2.1. Range-separated density functional theory for the ground state

The exact ground-state energy of an electronic system can be obtained variationally as follows, according to the Hohenberg–Kohn (HK) theorem [26]:

$$E_0 = \min_n \left\{ F[n] + \int d\mathbf{r}\, v_{ne}(\mathbf{r}) n(\mathbf{r}) \right\}, \tag{1}$$

where $v_{ne}(\mathbf{r})$ is the nuclear potential, $n(\mathbf{r})$ is a trial electron density and $F[n]$ is the universal Levy–Lieb (LL) functional defined by

$$F[n] = \min_{\Psi \to n} \langle \Psi | \hat{T} + \hat{W}_{ee} | \Psi \rangle, \tag{2}$$

where $\hat{T}$ is the kinetic energy operator and $\hat{W}_{ee}$ is the two-electron repulsion operator. In Kohn–Sham DFT [27] (KS-DFT), we consider a non-interacting system which has the same density as the physical one, and the wave

function is replaced by a Slater determinant $\Phi^{KS}[n]$. The universal LL functional becomes

$$F[n] = \langle \Phi^{KS}[n] | \hat{T} | \Phi^{KS}[n] \rangle + E_{Hxc}[n] = T_s[n] + E_{Hxc}[n], \tag{3}$$

where $E_{Hxc}[n]$ is the universal Hartree–exchange–correlation density functional and $T_s[n]$ is the non-interacting kinetic energy. An exact multi-determinantal extension of KS-DFT can be obtained by decomposing the two-electron repulsion into long-range and short-range parts, as proposed by Savin [20]. This decomposition is controlled by a parameter $\mu$:

$$w_{ee}(r_{12}) = \frac{1}{r_{12}} = w_{ee}^{lr,\mu}(r_{12}) + w_{ee}^{sr,\mu}(r_{12}),$$

$$w_{ee}^{lr,\mu}(r_{12}) = \mathrm{erf}(\mu r_{12})/r_{12} = \frac{2}{r_{12}\sqrt{\pi}} \int_0^{\mu r_{12}} e^{-t^2} dt, \tag{4}$$

where erf is the error function and $\mu \in [0, +\infty[$. The key idea in range-separated DFT is to treat the long-range interaction explicitly and to describe the short-range counterpart implicitly by means of a density functional, thus leading to the following expression for the universal LL functional:

$$F[n] = F^{lr,\mu}[n] + E_{Hxc}^{sr,\mu}[n], \tag{5}$$

where

$$\begin{aligned} F^{lr,\mu}[n] &= \min_{\Psi \to n} \langle \Psi | \hat{T} + \hat{W}_{ee}^{lr,\mu} | \Psi \rangle \\ &= \langle \Psi^\mu[n] | \hat{T} + \hat{W}_{ee}^{lr,\mu} | \Psi^\mu[n] \rangle. \end{aligned} \tag{6}$$

In analogy with KS-DFT, the short-range density functional can be decomposed as follows:

$$E_{Hxc}^{sr,\mu}[n] = E_H^{sr,\mu}[n] + E_x^{sr,\mu}[n] + E_c^{sr,\mu}[n], \tag{7}$$

where the short-range Hartree term is given by

$$E_H^{sr,\mu}[n] = \frac{1}{2} \int \int d\mathbf{r} d\mathbf{r}'\, n(\mathbf{r}) n(\mathbf{r}') w_{ee}^{sr,\mu}\left(|\mathbf{r} - \mathbf{r}'|\right), \tag{8}$$

the short-range exchange part is defined as

$$E_x^{sr,\mu}[n] = \langle \Phi^{KS}[n] | \hat{W}_{ee}^{sr,\mu} | \Phi^{KS}[n] \rangle - E_H^{sr,\mu}[n], \tag{9}$$

and the remaining short-range correlation part can be connected with the conventional (full-range) correlation functional as follows [28,29]:

$$\begin{aligned} E_c^{sr,\mu}[n] = E_c[n] &+ \langle \Phi^{KS}[n] | \hat{T} + \hat{W}_{ee}^{lr,\mu} | \Phi^{KS}[n] \rangle \\ &- \langle \Psi^\mu[n] | \hat{T} + \hat{W}_{ee}^{lr,\mu} | \Psi^\mu[n] \rangle. \end{aligned} \tag{10}$$

From the decomposition in Equation (5), we obtain the following expression for the exact ground-state energy:

$$
\begin{aligned}
E_0 &= \min_n \left\{ F^{\mathrm{lr},\mu}[n] + E^{\mathrm{sr},\mu}_{\mathrm{Hxc}}[n] + \int d\mathbf{r}\, v_{\mathrm{ne}}(\mathbf{r})n(\mathbf{r}) \right\}, \\
&= \min_{\Psi} \left\{ \langle \Psi | \hat{T} + \hat{W}^{\mathrm{lr},\mu}_{\mathrm{ee}} + \hat{V}_{\mathrm{ne}} | \Psi \rangle + E^{\mathrm{sr},\mu}_{\mathrm{Hxc}}[n_\Psi] \right\}, \\
&= \langle \Psi^\mu_0 | \hat{T} + \hat{W}^{\mathrm{lr},\mu}_{\mathrm{ee}} + \hat{V}_{\mathrm{ne}} | \Psi^\mu_0 \rangle + E^{\mathrm{sr},\mu}_{\mathrm{Hxc}}[n_{\Psi^\mu_0}],
\end{aligned}
\tag{11}
$$

where $\Psi^\mu_0$ is the exact minimising wave function which has the same density as the fully interacting ground-state wave function $\Psi_0$, and $\hat{V}_{\mathrm{ne}} = \int d\mathbf{r}\, v_{\mathrm{ne}}(\mathbf{r})\hat{n}(\mathbf{r})$, where $\hat{n}(\mathbf{r})$ is the density operator. It fulfils the following self-consistent equation:

$$
\hat{H}^\mu[n_{\Psi^\mu_0}] | \Psi^\mu_0 \rangle = \mathcal{E}^\mu_0 | \Psi^\mu_0 \rangle,
\tag{12}
$$

where

$$
\hat{H}^\mu[n_{\Psi^\mu_0}] = \hat{T} + \hat{W}^{\mathrm{lr},\mu}_{\mathrm{ee}} + \hat{V}_{\mathrm{ne}} + \int d\mathbf{r} \frac{\delta E^{\mathrm{sr},\mu}_{\mathrm{Hxc}}[n_{\Psi^\mu_0}]}{\delta n(\mathbf{r})} \hat{n}(\mathbf{r}).
\tag{13}
$$

Range separation leads to an exact combination of wave function theory and KS-DFT. The former is recovered when $\mu \to +\infty$, while the latter is recovered when $\mu = 0$. Note that the spectrum $\{\mathcal{E}^\mu_k\}_{k=0,1,2,\dots}$ of the auxiliary long-range interacting Hamiltonian $\hat{H}^\mu[n_{\Psi^\mu_0}]$ can be used as a starting point for approaching the exact physical spectrum. This can be achieved within the time-dependent linear response (LR) regime [30]. In this paper, we will focus on time-independent approaches. One of them, which was initially proposed by Savin [23], consists in using the expansion of the auxiliary energies for large $\mu$ values:

$$
\mathcal{E}^\mu_k = E_k - \frac{\mu}{2} \frac{\partial \mathcal{E}^\mu_k}{\partial \mu} + \mathcal{O}\left(\frac{1}{\mu^3}\right),
\tag{14}
$$

where $E_k$ is the exact $k$th physical energy, thus leading to the extrapolated energy through second order in $1/\mu$ [23–25]:

$$
\mathcal{E}^\mu_{E,k} = \mathcal{E}^\mu_k + \frac{\mu}{2} \frac{\partial \mathcal{E}^\mu_k}{\partial \mu}.
\tag{15}
$$

As discussed in Section 2.5, such an extrapolation scheme can also be applied to range-separated ensemble energies in order to obtain more accurate excitation energies.

## 2.2. Ensemble density functional theory

In contrast to KS-DFT, ensemble DFT allows for the calculation of excitation energies. This is achieved by assigning weights to ground and excited states so that the weighted sum of energies and densities, referred to as ensemble energy and ensemble density, respectively, can be constructed. Let us consider an ensemble consisting of $M$ states with ensemble weights $\mathbf{w} \equiv (w_0, w_1, \dots, w_{M-1})$ ordered as $w_0 \geq w_1 \geq \cdots \geq w_{M-1}$. Note that Boltzmann weights can be used [21], but it is not compulsory. The summation constraint $\sum_{k=0}^{M-1} w_k = 1$ will be used in the following so that the ensemble density integrates to the number $N$ of electrons. According to the Gross–Oliveira–Kohn (GOK) variational principle [6],

$$
E^{\mathbf{w}} \leq \mathrm{Tr}[\hat{\gamma}^{\mathbf{w}} \hat{H}],
\tag{16}
$$

where Tr denotes the trace, $\hat{H} = \hat{T} + \hat{W}_{\mathrm{ee}} + \hat{V}_{\mathrm{ne}}$ is the physical Hamiltonian, and $\hat{\gamma}^{\mathbf{w}}$ is a trial ensemble density matrix constructed from a set of $M$ orthonormal trial wave functions $\{\overline{\Psi}_k\}_{0 \leq k \leq M-1}$:

$$
\hat{\gamma}^{\mathbf{w}} = \sum_{k=0}^{M-1} w_k | \overline{\Psi}_k \rangle \langle \overline{\Psi}_k |.
\tag{17}
$$

The exact ensemble energy is the lower bound in Equation (16):

$$
E^{\mathbf{w}} = \mathrm{Tr}[\hat{\Gamma}^{\mathbf{w}} \hat{H}] = \sum_{k=0}^{M-1} w_k E_k,
\tag{18}
$$

where $\hat{\Gamma}^{\mathbf{w}} = \sum_{k=0}^{M-1} w_k | \Psi_k \rangle \langle \Psi_k |$ is the exact physical ensemble density matrix, $\Psi_k$ is the exact $k$th eigenfunction of $\hat{H}$, and $E_0 \leq E_1 \leq \cdots \leq E_{M-1}$. The GOK variational principle extends the HK theorem to ensembles [7], so that the ensemble energy can be obtained variationally as follows:

$$
E^{\mathbf{w}} = \min_n \left\{ F^{\mathbf{w}}[n] + \int d\mathbf{r}\, v_{\mathrm{ne}}(\mathbf{r})n(\mathbf{r}) \right\},
\tag{19}
$$

where the universal LL ensemble functional equals

$$
F^{\mathbf{w}}[n] = \min_{\hat{\gamma}^{\mathbf{w}} \to n} \{ \mathrm{Tr}[\hat{\gamma}^{\mathbf{w}}(\hat{T} + \hat{W}_{\mathrm{ee}})] \}.
\tag{20}
$$

Note that, in Equation (20), the minimisation is restricted to ensemble density matrices with ensemble density $n$:

$$
\mathrm{Tr}[\hat{\gamma}^{\mathbf{w}} \hat{n}(\mathbf{r})] = n_{\hat{\gamma}^{\mathbf{w}}}(\mathbf{r}) = n(\mathbf{r}).
\tag{21}
$$

Note also that the minimising density in Equation (19) is the exact ensemble density $n_{\hat{\Gamma}^{\mathbf{w}}}(\mathbf{r}) = \sum_{k=0}^{M-1} w_k n_{\Psi_k}(\mathbf{r})$.

By analogy with KS-DFT, Gross et al. [7] considered the following partitioning of the LL ensemble functional:

$$F^{\mathbf{w}}[n] = T_s^{\mathbf{w}}[n] + E_{\text{Hxc}}^{\mathbf{w}}[n], \qquad (22)$$

where $T_s^{\mathbf{w}}[n]$ is the non-interacting ensemble kinetic energy:

$$T_s^{\mathbf{w}}[n] = \min_{\hat{\gamma}^{\mathbf{w}} \to n} \{\text{Tr}[\hat{\gamma}^{\mathbf{w}}\hat{T}]\}$$
$$= \text{Tr}[\hat{\Gamma}_s^{\mathbf{w}}[n]\hat{T}], \qquad (23)$$

$\hat{\Gamma}_s^{\mathbf{w}}[n]$ denotes the non-interacting ensemble density matrix with density $n$ and $E_{\text{Hxc}}^{\mathbf{w}}[n]$ is the weight-dependent Hartree–exchange–correlation ensemble functional. The conventional (weight-independent) ground-state Hartree functional is usually employed [7], thus leading to the following decomposition:

$$E_{\text{Hxc}}^{\mathbf{w}}[n] = E_{\text{H}}[n] + E_{\text{x}}^{\mathbf{w}}[n] + E_{\text{c}}^{\mathbf{w}}[n], \qquad (24)$$

where the exact ensemble exchange density functional energy is defined in terms of the non-interacting ensemble density matrix:

$$E_{\text{x}}^{\mathbf{w}}[n] = \text{Tr}[\hat{\Gamma}_s^{\mathbf{w}}[n]\hat{W}_{\text{ee}}] - E_{\text{H}}[n]. \qquad (25)$$

Note that the Hartree term will always contain the so-called ghost-interaction errors [31] when computed with an ensemble density, simply because it is quadratic in the input density $n$. The exact ensemble exchange functional removes such errors, as readily seen in Equation (25). Since, in practice, approximate functionals are used, ghost interactions might be significant, thus requiring correction schemes [17,31,32]. This will be discussed further in Section 6, in the context of range-separated ensemble DFT.

By using the KS partitioning in Equation (22), the exact ensemble energy becomes

$$E^{\mathbf{w}} = \min_n \left\{ T_s^{\mathbf{w}}[n] + \int d\mathbf{r}\, v_{\text{ne}}(\mathbf{r})n(\mathbf{r}) + E_{\text{Hxc}}^{\mathbf{w}}[n] \right\}, \qquad (26)$$

or, equivalently,

$$E^{\mathbf{w}} = \min_{\hat{\gamma}^{\mathbf{w}}} \left\{ \text{Tr}[\hat{\gamma}^{\mathbf{w}}(\hat{T} + \hat{V}_{\text{ne}})] + E_{\text{Hxc}}^{\mathbf{w}}[n_{\hat{\gamma}^{\mathbf{w}}}] \right\}. \qquad (27)$$

The minimising non-interacting GOK ensemble density matrix,

$$\hat{\Gamma}_s^{\mathbf{w}} = \sum_{k=0}^{M-1} w_k |\Phi_k^{\mathbf{w}}\rangle\langle\Phi_k^{\mathbf{w}}|, \qquad (28)$$

reproduces the exact physical ensemble density: $n_{\hat{\Gamma}^{\mathbf{w}}}(\mathbf{r}) = n_{\hat{\Gamma}^{\mathbf{w}}}(\mathbf{r})$. Finally, by considering the Lagrangian [22]

$$\mathcal{L}^{\mathbf{w}}[\hat{\gamma}^{\mathbf{w}}] = \text{Tr}[\hat{\gamma}^{\mathbf{w}}(\hat{T} + \hat{V}_{\text{ne}})] + E_{\text{Hxc}}^{\mathbf{w}}[n_{\hat{\gamma}^{\mathbf{w}}}]$$
$$+ \sum_{k=0}^{M-1} w_k \mathcal{E}_k^{\mathbf{w}} \left(1 - \langle\overline{\Psi}_k|\overline{\Psi}_k\rangle\right), \qquad (29)$$

where $\mathcal{E}_k^{\mathbf{w}}$ are Lagrange multipliers associated with the normalisation of the trial wave functions $\overline{\Psi}_k$ from which the ensemble density matrix is built, we obtain from the stationarity condition $\delta\mathcal{L}^{\mathbf{w}}[\hat{\Gamma}_s^{\mathbf{w}}] = 0$ the self-consistent GOK-DFT equations [7]:

$$\left(\hat{T} + \hat{V}_{\text{ne}} + \int d\mathbf{r}\frac{\delta E_{\text{Hxc}}^{\mathbf{w}}[n_{\hat{\Gamma}_s^{\mathbf{w}}}]}{\delta n(\mathbf{r})}\hat{n}(\mathbf{r})\right)|\Phi_k^{\mathbf{w}}\rangle = \mathcal{E}_k^{\mathbf{w}}|\Phi_k^{\mathbf{w}}\rangle. \qquad (30)$$

### 2.3. Range-separated ensemble density functional theory

In analogy with ground-state range-separated DFT, range separation can be introduced into the LL ensemble functional [13,21], thus leading to the following decomposition:

$$F^{\mathbf{w}}[n] = F^{\text{lr},\mu,\mathbf{w}}[n] + E_{\text{Hxc}}^{\text{sr},\mu,\mathbf{w}}[n], \qquad (31)$$

where

$$F^{\text{lr},\mu,\mathbf{w}}[n] = \min_{\hat{\gamma}^{\mathbf{w}} \to n} \left\{\text{Tr}[\hat{\gamma}^{\mathbf{w}}(\hat{T} + \hat{W}_{\text{ee}}^{\text{lr},\mu})]\right\}$$
$$= \text{Tr}[\hat{\Gamma}^{\mu,\mathbf{w}}[n](\hat{T} + \hat{W}_{\text{ee}}^{\text{lr},\mu})]. \qquad (32)$$

The short-range ensemble density functional is both $\mu$- and $\mathbf{w}$-dependent. In analogy with GOK-DFT [7], it can be partitioned as follows:

$$E_{\text{Hxc}}^{\text{sr},\mu,\mathbf{w}}[n] = E_{\text{H}}^{\text{sr},\mu}[n] + E_{\text{x}}^{\text{sr},\mu,\mathbf{w}}[n] + E_{\text{c}}^{\text{sr},\mu,\mathbf{w}}[n], \quad (33)$$

where the ground-state ($\mathbf{w}$-independent) short-range Hartree functional defined in Equation (8) is used. The exact short-range exchange ensemble energy can be expressed in terms of the non-interacting ensemble density matrix (see Equation (23)) as

$$E_{\text{x}}^{\text{sr},\mu,\mathbf{w}}[n] = \text{Tr}[\hat{\Gamma}_s^{\mathbf{w}}[n]\hat{W}_{\text{ee}}^{\text{sr},\mu}] - E_{\text{H}}^{\text{sr},\mu}[n], \qquad (34)$$

and, according to Equations (22), (24), (25), (31), and (32), the complementary short-range correlation energy for the ensemble can be related with the conventional (full-range) correlation energy as follows:

$$E_{\text{c}}^{\text{sr},\mu,\mathbf{w}}[n] = E_{\text{c}}^{\mathbf{w}}[n] + \text{Tr}[\hat{\Gamma}_s^{\mathbf{w}}[n](\hat{T} + \hat{W}_{\text{ee}}^{\text{lr},\mu})]$$
$$- \text{Tr}[\hat{\Gamma}^{\mu,\mathbf{w}}[n](\hat{T} + \hat{W}_{\text{ee}}^{\text{lr},\mu})]. \qquad (35)$$

Note that Equation (10) is recovered when the ensemble reduces to the ground state ($w_0 = 1$). Note also that, as in GOK-DFT, the exact short-range ensemble energy removes the ghost-interaction errors introduced in the short-range Hartree energy (see Equations (25) and (34)). In practice [21,22], the use of (semi-) local ground-state short-range exchange density functionals cannot, in principle, remove such errors. In Section 6, an alternative decomposition of the short-range ensemble exchange–correlation energy will be proposed and discussed. The latter provides a rigorous framework for performing ghost-interaction-free multi-determinant range-separated ensemble DFT calculations. Work is currently in progress in this direction.

Returning to the range-separated LL ensemble functional expression in Equation (31), we finally obtain from Equation (19) the following exact expression for the ensemble energy:

$$
\begin{aligned}
E^{\mathbf{w}} &= \min_{\hat{\gamma}^{\mathbf{w}}} \left\{ \mathrm{Tr}\big[\hat{\gamma}^{\mathbf{w}}\big(\hat{T} + \hat{W}_{\mathrm{ee}}^{\mathrm{lr},\mu} + \hat{V}_{\mathrm{ne}}\big)\big] + E_{\mathrm{Hxc}}^{\mathrm{sr},\mu,\mathbf{w}}[n_{\hat{\gamma}^{\mathbf{w}}}] \right\} \\
&= \mathrm{Tr}\big[\hat{\Gamma}^{\mu,\mathbf{w}}\big(\hat{T} + \hat{W}_{\mathrm{ee}}^{\mathrm{lr},\mu} + \hat{V}_{\mathrm{ne}}\big)\big] + E_{\mathrm{Hxc}}^{\mathrm{sr},\mu,\mathbf{w}}[n_{\hat{\Gamma}^{\mu,\mathbf{w}}}],
\end{aligned}
$$
(36)

where the minimising long-range-interacting ensemble density matrix $\hat{\Gamma}^{\mu,\mathbf{w}} = \sum_{k=0}^{M-1} w_k |\Psi_k^{\mu,\mathbf{w}}\rangle \langle \Psi_k^{\mu,\mathbf{w}}|$ reproduces the exact physical ensemble density: $n_{\hat{\Gamma}^{\mu,\mathbf{w}}}(\mathbf{r}) = n_{\hat{\Gamma}^{\mathbf{w}}}(\mathbf{r})$. This density matrix fulfils the following self-consistent equation, in analogy with Equation (30):

$$
\begin{aligned}
&\left( \hat{T} + \hat{W}_{\mathrm{ee}}^{\mathrm{lr},\mu} + \hat{V}_{\mathrm{ne}} + \int d\mathbf{r} \frac{\delta E_{\mathrm{Hxc}}^{\mathrm{sr},\mu,\mathbf{w}}[n_{\hat{\Gamma}^{\mu,\mathbf{w}}}]}{\delta n(\mathbf{r})} \hat{n}(\mathbf{r}) \right) |\Psi_k^{\mu,\mathbf{w}}\rangle \\
&= \mathcal{E}_k^{\mu,\mathbf{w}} |\Psi_k^{\mu,\mathbf{w}}\rangle.
\end{aligned}
$$
(37)

When $\mu \to +\infty$, we recover the Schrödinger equation and, when $\mu = 0$, GOK-DFT equations are obtained.

Let us now consider the particular case of two non-degenerate states. The ensemble weights are then reduced to two weights, $w_0$ for the ground state and $w_1$ for the first excited state. Both can be expressed in terms of a single weight $w$:

$$
w_0 = 1 - w, \quad w_1 = w,
$$
(38)

with $w \in [0, 1/2]$. The exact ensemble energy is a linear function of $w$,

$$
E^w = (1 - w)E_0 + wE_1,
$$
(39)

and the excitation energy $\omega$ is simply the first derivative of the ensemble energy with respect to $w$:

$$
\begin{aligned}
\omega &= \frac{dE^w}{dw}, \\
&= E_1 - E_0.
\end{aligned}
$$
(40)

Linearity in $w$ also enables to obtain the excitation energy by linear interpolation between ground state and equi-ensemble energies:

$$
\begin{aligned}
\omega &= 2(E^{w=1/2} - E^{w=0}) \\
&= 2(E^{w=1/2} - E_0).
\end{aligned}
$$
(41)

In this particular case of a two-state ensemble, the exact range-separated ensemble energy in Equation (36) can be rewritten as

$$
\begin{aligned}
E^w &= (1 - w)\langle \Psi_0^{\mu,w} | \hat{T} + \hat{W}_{\mathrm{ee}}^{\mathrm{lr},\mu} + \hat{V}_{\mathrm{ne}} | \Psi_0^{\mu,w}\rangle \\
&\quad + w\langle \Psi_1^{\mu,w} | \hat{T} + \hat{W}_{\mathrm{ee}}^{\mathrm{lr},\mu} + \hat{V}_{\mathrm{ne}} | \Psi_1^{\mu,w}\rangle + E_{\mathrm{Hxc}}^{\mathrm{sr},\mu,w}[n_{\hat{\Gamma}^{\mu,w}}],
\end{aligned}
$$
(42)

or, equivalently (see Equation (37)),

$$
\begin{aligned}
E^w &= (1 - w)\mathcal{E}_0^{\mu,w} + w\mathcal{E}_1^{\mu,w} \\
&\quad - \int d\mathbf{r} \frac{\delta E_{\mathrm{Hxc}}^{\mathrm{sr},\mu,w}[n_{\hat{\Gamma}^{\mu,w}}]}{\delta n(\mathbf{r})} n_{\hat{\Gamma}^{\mu,w}}(\mathbf{r}) + E_{\mathrm{Hxc}}^{\mathrm{sr},\mu,w}[n_{\hat{\Gamma}^{\mu,w}}],
\end{aligned}
$$
(43)

where the auxiliary ensemble density equals the physical one:

$$
n_{\hat{\Gamma}^{\mu,w}}(\mathbf{r}) = (1 - w)n_{\Psi_0^{\mu,w}}(\mathbf{r}) + wn_{\Psi_1^{\mu,w}}(\mathbf{r}) = n_{\hat{\Gamma}^w}(\mathbf{r}).
$$
(44)

Using Equation (40) leads to the following exact expression for the first excitation energy [13,22]:

$$
\begin{aligned}
\omega &= \mathcal{E}_1^{\mu,w} - \mathcal{E}_0^{\mu,w} + \left.\frac{\partial E_{\mathrm{Hxc}}^{\mathrm{sr},\mu,w}[n]}{\partial w}\right|_{n=n_{\hat{\Gamma}^w}} \\
&= \Delta\mathcal{E}^{\mu,w} + \Delta_{\mathrm{xc}}^{\mu,w},
\end{aligned}
$$
(45)

where $\Delta\mathcal{E}^{\mu,w}$ is the auxiliary (weight-dependent) excitation energy and $\Delta_{\mathrm{xc}}^{\mu,w}$ is the short-range exchange–correlation derivative discontinuity (the short-range Hartree term does not depend on the weight as shown in Equation (33)). As readily seen from Equation (45), the auxiliary excitation energy is in principle not equal to the physical one.

## 2.4. Linear interpolation method

The construction of approximate ensemble exchange–correlation functionals is already a challenge in the context of GOK-DFT [9,11,12,15]. In the case of range-separated ensemble DFT, an exact adiabatic connection formula has been derived by Franck and Fromager [13], but no approximations have been developed so far. The simplest approximation consists in using the (weight-independent) ground-state short-range functional [21,22],

$$E_{\mathrm{Hxc}}^{\mathrm{sr},\mu,\mathbf{w}}[n] \to E_{\mathrm{Hxc}}^{\mathrm{sr},\mu}[n]. \qquad (46)$$

We shall refer to this approximation as *weight-independent density functional approximation* (WIDFA). The range-separated ensemble energy within WIDFA can be expressed as

$$
\begin{aligned}
\tilde{E}^{\mu,\mathbf{w}} &= \min_{\hat{\gamma}^{\mathbf{w}}} \left\{ \mathrm{Tr}\big[\hat{\gamma}^{\mathbf{w}}(\hat{T} + \hat{W}_{\mathrm{ee}}^{\mathrm{lr},\mu} + \hat{V}_{\mathrm{ne}})\big] + E_{\mathrm{Hxc}}^{\mathrm{sr},\mu}[n_{\hat{\gamma}^{\mathbf{w}}}] \right\} \\
&= \mathrm{Tr}\big[\hat{\gamma}^{\mu,\mathbf{w}}(\hat{T} + \hat{W}_{\mathrm{ee}}^{\mathrm{lr},\mu} + \hat{V}_{\mathrm{ne}})\big] + E_{\mathrm{Hxc}}^{\mathrm{sr},\mu}[n_{\hat{\gamma}^{\mu,\mathbf{w}}}],
\end{aligned}
\qquad (47)
$$

where the minimising ensemble density matrix $\hat{\gamma}^{\mu,\mathbf{w}} = \sum_{k=0}^{M-1} w_k |\tilde{\Psi}_k^{\mu,\mathbf{w}}\rangle\langle\tilde{\Psi}_k^{\mu,\mathbf{w}}|$ fulfils the following set of self-consistent equations:

$$
\begin{aligned}
&\left(\hat{T} + \hat{W}_{\mathrm{ee}}^{\mathrm{lr},\mu} + \hat{V}_{\mathrm{ne}} + \int d\mathbf{r} \frac{\delta E_{\mathrm{Hxc}}^{\mathrm{sr},\mu}[n_{\hat{\gamma}^{\mu,\mathbf{w}}}]}{\delta n(\mathbf{r})} \hat{n}(\mathbf{r})\right) |\tilde{\Psi}_k^{\mu,\mathbf{w}}\rangle \\
&= \tilde{\mathcal{E}}_k^{\mu,\mathbf{w}} |\tilde{\Psi}_k^{\mu,\mathbf{w}}\rangle, \quad 0 \le k \le M-1.
\end{aligned}
\qquad (48)
$$

Note that the exact physical ensemble density matrix $\hat{\Gamma}^{\mathbf{w}}$ and the exact ensemble energy $E^{\mathbf{w}}$ are recovered from Equation (47) when $\mu \to +\infty$.

In the particular case of a two-state ensemble with weight $w$, the WIDFA excitation energy defined as the derivative of the WIDFA ensemble energy with respect to $w$ reduces to the approximate auxiliary excitation energy [22]:

$$\omega_{\mathrm{WIDFA}}^{\mu,w} = \frac{d\tilde{E}^{\mu,w}}{dw} = \tilde{\mathcal{E}}_1^{\mu,w} - \tilde{\mathcal{E}}_0^{\mu,w} = \Delta\tilde{\mathcal{E}}^{\mu,w}. \quad (49)$$

As a result, it is both $\mu$- and $w$-dependent. The ambiguity in the choice of the ensemble weight for computing excitation energies can be overcome by means of linear interpolations between equi-ensembles [22]. In other words, the exact linearly interpolated expression in Equation (41) is used rather than the first-order-derivative-based expression in Equation (40) in order to compute approximate excitation energies. Both choices are of course equivalent if exact wave functions and functionals

are used. This LIM leads, for two states, to the following simple $\mu$-dependent (but $w$-independent) expression:

$$\omega_{\mathrm{LIM}}^{\mu} = 2(\tilde{E}^{\mu,1/2} - \tilde{E}^{\mu,0}). \qquad (50)$$

Interestingly, LIM enables to define an effective derivative discontinuity that exhibits, in helium for example, similar variations in $w$ as the exact derivative discontinuity [22]:

$$\Delta_{\mathrm{eff}}^{\mu,w} = \omega_{\mathrm{LIM}}^{\mu} - \Delta\tilde{\mathcal{E}}^{\mu,w} = \omega_{\mathrm{LIM}}^{\mu} - \omega_{\mathrm{WIDFA}}^{\mu,w}. \qquad (51)$$

Note that $\Delta_{\mathrm{eff}}^{\mu,w} \to 0$ when $\mu \to +\infty$. As a result, the extrapolation method of Savin [23] cannot be used in this context for obtaining more accurate variations of the short-range derivative discontinuity with $w$ for a fixed and finite value of $\mu$.

Let us finally mention that LIM can be easily extended to higher excitations and degenerate states by considering the WIDFA ensemble energy (denoted $\tilde{E}_I^{\mu,w}$ in the following) defined from the following ensemble weights:

$$w_k = \begin{cases} \frac{1 - wg_I}{M_{I-1}} & 0 \le k \le M_{I-1} - 1, \\ w & M_{I-1} \le k \le M_I - 1, \end{cases} \qquad (52)$$

where

$$
\begin{aligned}
&0 \le w \le \frac{1}{M_I}, \\
&M_I = \sum_{L=0}^{I} g_L,
\end{aligned}
\qquad (53)
$$

and $g_L$ is the degeneracy of the $L$th energy. The $I$th LIM excitation energy can then be obtained as follows [22]:

$$\omega_{\mathrm{LIM},I}^{\mu} = \frac{M_I}{g_I}\left(\tilde{E}_I^{\mu,1/M_I} - \tilde{E}_{I-1}^{\mu,1/M_{I-1}}\right) + \frac{1}{M_{I-1}}\sum_{K=1}^{I-1} g_K \omega_{\mathrm{LIM},K}^{\mu}. \qquad (54)$$

From the equality $\tilde{E}_{I-1}^{\mu,1/M_{I-1}} = \tilde{E}_I^{\mu,0}$, it becomes clear from Equation (54) that LIM interpolates the ensemble energy between equi-ensembles. In the particular case of three non-degenerate states, the second LIM excitation energy equals, with the notations of Equation (50),

$$\omega_{\mathrm{LIM},2}^{\mu} = 3\big(\tilde{E}_2^{\mu,1/3} - \tilde{E}^{\mu,1/2}\big) + \frac{1}{2}\omega_{\mathrm{LIM}}^{\mu}. \qquad (55)$$

## 2.5. Extrapolating excitation energies from range-separated ensemble energies

In the spirit of Savin and co-workers [23–25], we propose to extrapolate physical excitation energies from the approximate LIM excitation energies. For that purpose,

let us introduce $\eta = 1/\mu$ and consider the $\mu \to +\infty$ limit or, equivalently, $\eta \to 0$. The WIDFA range-separated ensemble energy in Equation (47) can be expanded through second order in $\eta$ as follows:

$$\tilde{E}^{1/\eta,\mathbf{w}} = E^{\mathbf{w}} + \tilde{E}^{(-1),\mathbf{w}}\eta + \tilde{E}^{(-2),\mathbf{w}}\eta^2 + \mathcal{O}(\eta^3), \quad (56)$$

where, according to the Hellmann–Feynman theorem,

$$\tilde{E}^{(-1),\mathbf{w}} = \left.\frac{d\tilde{E}^{1/\eta,\mathbf{w}}}{d\eta}\right|_{\eta=0}$$
$$= \mathrm{Tr}\left[\hat{\Gamma}^{\mathbf{w}}\left.\frac{\partial\hat{W}_{ee}^{lr,1/\eta}}{\partial\eta}\right|_{\eta=0}\right] + \left.\frac{\partial E_{\mathrm{Hxc}}^{sr,1/\eta}[n_{\hat{\Gamma}^{\mathbf{w}}}]}{\partial\eta}\right|_{\eta=0}. \quad (57)$$

For large $\mu$ values, the short-range density functional energy can be expanded as follows [28,33]:

$$E_{\mathrm{Hxc}}^{sr,\mu}[n] = \frac{1}{\mu^2}E_{\mathrm{Hxc}}^{sr,(-2)}[n] + \mathcal{O}\left(\frac{1}{\mu^3}\right). \quad (58)$$

Therefore, the second term on the right-hand side of Equation (57) equals zero. Moreover, according to Equation (4),

$$\frac{\partial w_{ee}^{lr,1/\eta}(r_{12})}{\partial\eta} = -\frac{2}{\eta^2\sqrt{\pi}}e^{-r_{12}^2/\eta^2}, \quad (59)$$

so that

$$\mathrm{Tr}\left[\hat{\Gamma}^{\mathbf{w}}\frac{\partial\hat{W}_{ee}^{lr,1/\eta}}{\partial\eta}\right] = -8\sqrt{\pi}\int_0^{+\infty}\frac{r_{12}^2}{\eta^2}e^{-r_{12}^2/\eta^2}f_{\hat{\Gamma}^{\mathbf{w}}}(r_{12})dr_{12}, \quad (60)$$

where $f_{\hat{\Gamma}^{\mathbf{w}}}(r_{12}) = \sum_k w_k f_{\Psi_k}(r_{12})$ is the exact physical ensemble intracule density (see, for example, [33]). It becomes clear from Equation (60) that the first term on the right-hand side of Equation (57) is also equal to zero, thus leading to $\tilde{E}^{(-1),\mathbf{w}} = 0$. In conclusion, for large $\mu$ values, the deviation of the WIDFA ensemble energy from the exact one is at least of second order in $1/\mu$:

$$\tilde{E}^{\mu,\mathbf{w}} = E^{\mathbf{w}} + \frac{1}{\mu^2}\tilde{E}^{(-2),\mathbf{w}} + \mathcal{O}\left(\frac{1}{\mu^3}\right), \quad (61)$$

or, equivalently,

$$E^{\mathbf{w}} = \tilde{E}^{\mu,\mathbf{w}} + \frac{\mu}{2}\frac{\partial\tilde{E}^{\mu,\mathbf{w}}}{\partial\mu} + \mathcal{O}\left(\frac{1}{\mu^3}\right). \quad (62)$$

A similar Taylor expansion can also be obtained for the auxiliary energies:

$$E_k = \tilde{\mathcal{E}}_k^{\mu,\mathbf{w}} + \frac{\mu}{2}\frac{\partial\tilde{\mathcal{E}}_k^{\mu,\mathbf{w}}}{\partial\mu} + \mathcal{O}\left(\frac{1}{\mu^3}\right). \quad (63)$$

Thus, we obtain from Equations (62) and (63) the following extrapolated expressions through second order in $1/\mu$ for the ensemble energy,

$$\tilde{E}_E^{\mu,\mathbf{w}} = \tilde{E}^{\mu,\mathbf{w}} + \frac{\mu}{2}\frac{\partial\tilde{E}^{\mu,\mathbf{w}}}{\partial\mu}, \quad (64)$$

and the individual energies,

$$\tilde{\mathcal{E}}_{E,k}^{\mu,\mathbf{w}} = \tilde{\mathcal{E}}_k^{\mu,\mathbf{w}} + \frac{\mu}{2}\frac{\partial\tilde{\mathcal{E}}_k^{\mu,\mathbf{w}}}{\partial\mu}, \quad (65)$$

respectively. Note that Savin's extrapolation scheme (see Equation (15)) is recovered from Equation (65) in the ground-state density limit ($w_0 = 1$).

Within LIM, the $I$th excitation energy $\omega_{\mathrm{LIM},I}^{\mu}$ is simply expressed as the linear combination of range-separated equi-ensemble energies that are all computed at the WIDFA level (see Equation (54)). This expression becomes exact when $\mu \to +\infty$. Consequently, the exact $I$th excitation energy $\omega_I$ can be connected to the approximate LIM one as follows:

$$\omega_{\mathrm{LIM},I}^{\mu} = \omega_I + \frac{1}{\mu^2}\omega_{\mathrm{LIM},I}^{(-2)} + \mathcal{O}\left(\frac{1}{\mu^3}\right), \quad (66)$$

or, equivalently,

$$\omega_I = \omega_{\mathrm{LIM},I}^{\mu} + \frac{\mu}{2}\frac{\partial\omega_{\mathrm{LIM},I}^{\mu}}{\partial\mu} + \mathcal{O}\left(\frac{1}{\mu^3}\right), \quad (67)$$

thus leading to the extrapolated LIM (ELIM) excitation energy expression through second order in $1/\mu$,

$$\omega_{\mathrm{ELIM},I}^{\mu} = \omega_{\mathrm{LIM},I}^{\mu} + \frac{\mu}{2}\frac{\partial\omega_{\mathrm{LIM},I}^{\mu}}{\partial\mu}. \quad (68)$$

As illustrated in Figure 1 for He and $H_2$, the LIM excitation energy does vary as $\mu^{-2}$ when $\mu$ is large, thus showing that the second-order term in Equation (66) is not zero.

Let us finally mention that better extrapolations can be obtained by considering higher order derivatives in $\mu$ [25], but this is left for future work.
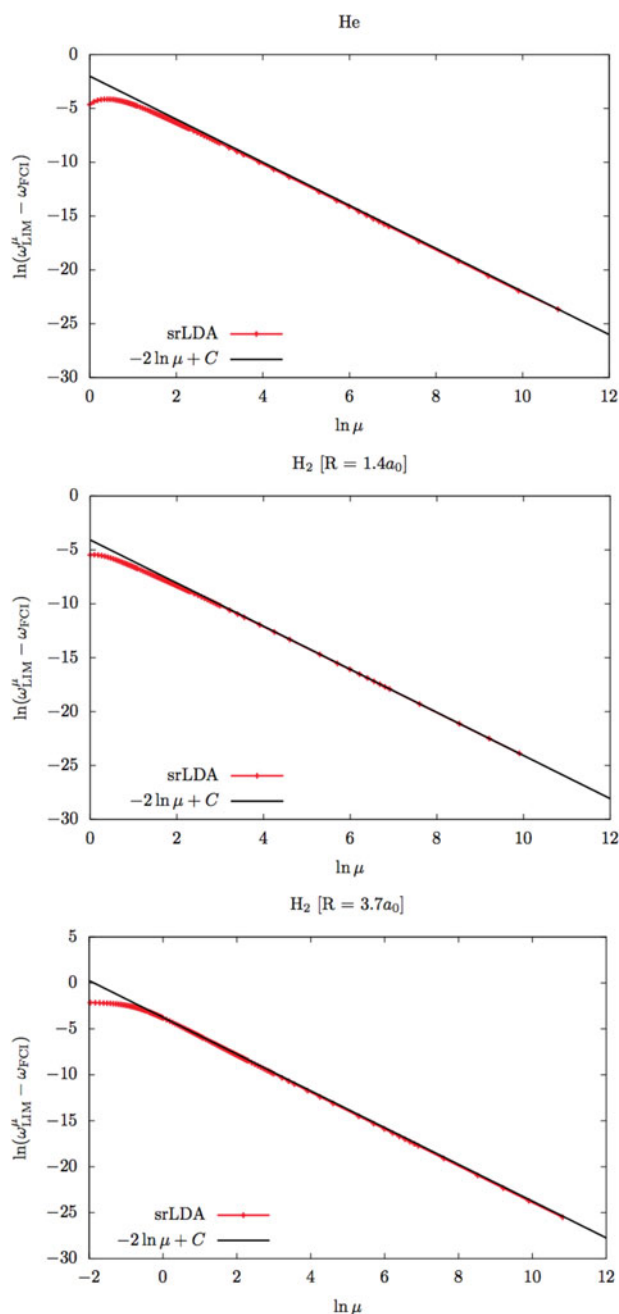
**Figure 1.** Graphical illustration of Equation (66) for two-state ensembles: $\{1^1S, 2^1S\}$ in He (top panel), $\{1^1\Sigma_g^+, 2^1\Sigma_g^+\}$ in $H_2$ at equilibrium (middle panel) and stretched (bottom panel) geometries. See text for further details.

## 3. Summary

In this section, we give a summary of all the approximate methods introduced previously and whose performance is discussed in Section 5. All of them rely on the range separation of the two-electron repulsion that is controlled by the parameter $\mu$ in the error function. A typical value is 0.4 [34] but its influence on the results will be investigated in details as follows. Note that, when $\mu = 0$, standard KS-DFT is recovered. On the other hand, wave

function theory is obtained when $\mu \to +\infty$. For intermediate values, the long-range interaction is treated with wave-function-based methods (full configuration interaction (FCI) will be used in this work) and short-range interactions are described by a complementary $\mu$-dependent density functional (a local functional will be used in this work). Range-separated DFT can be extended to excited states by means of ensembles. In the particular case of the first excitation, which is mainly discussed in the paper, the ensemble consists of the ground-state and first-excited-state wave functions. A weight $w$, which can vary from 0 to 1/2, is assigned to the latter. The weight associated to the ground state is $(1 - w)$. The exact ensemble energy, which is nothing but the weighted sum of the ground-state and first-excited-state energies, is linear in $w$. Therefore, its range-separated expression should also be linear in $w$ (and $\mu$-independent) if the exact $w$-dependent short-range ensemble functional were used. Note that, for a given $\mu$ value, ground-state range-separated DFT is recovered when $w = 0$. Returning to the short-range functional for the ensemble, a simple approximation consists in employing ground-state short-range functionals (a local one in our case) which has, therefore, no weight dependence. As a result, the approximate range-separated ensemble energy becomes both $\mu$- and $w$-dependent and, for a given $\mu$ value, it exhibits curvature in $w$. Of course, this is not the case in the exact theory so that the derivative of the ensemble energy with respect to $w$ is $w$-independent and equal to the exact excitation energy. The definition of approximate excitation energies is then not trivial since the derivative of the range-separated ensemble energy, which is referred to as auxiliary excitation energy, varies with $w$. LIM is a way to remove this weight dependence, simply by constructing, for a given $\mu$ value, the linear interpolation between the ground state and the equi-ensemble ($w = 1/2$). The slope of the linearly interpolated range-separated ensemble energy gives an approximate excitation energy which is weight-independent by construction. Of course, it still depends on $\mu$. When $\mu \to +\infty$, both auxiliary and LIM excitation energies become exact. Therefore, the extrapolation technique of Savin [23] can be applied in this context, thus leading for LIM to the ELIM approach. The method can be generalised to an arbitrary number of states. An example will be given for three states in $H_2$ along the bond-breaking coordinate.

## 4. Computational details

Extrapolated auxiliary and LIM excitation energies (see Equations (65) and (68)) have been computed with a development version of the DALTON program package [35,36]. Only the spin-independent short-range

local density approximation (srLDA) [20,37] has been used. It was shown in a previous work [22] that the short-range Perdew–Burke–Ernzerhof-type functional of Goll et al. [38] gives rather similar results, at least for the systems considered in this work. Basis sets are aug-cc-pVQZ [39,40]. Orbital relaxation and long-range correlation effects have been treated self-consistently at the FCI level. Calculations have been performed on He and Be atoms as well as $H_2$ and $HeH^+$ molecules. For Be, the 1s orbital was kept inactive. The following two-state singlet ensembles have been studied: $\{1^1S, 2^1S\}$ for He and Be, $\{1^1\Sigma^+, 2^1\Sigma^+\}$ for the stretched $HeH^+$ molecule ($R = 8.0$ a$_0$), and $\{1^1\Sigma_g^+, 2^1\Sigma_g^+\}$ for $H_2$ at equilibrium ($R = 1.4$ a$_0$) and stretched ($R = 3.7$ a$_0$) geometries. In addition, the three-state singlet ensemble $\{1^1\Sigma_g^+, 2^1\Sigma_g^+, 3^1\Sigma_g^+\}$ in $H_2$ has been considered along the bond-breaking coordinate. In the latter case, comparison is made with time-dependent multi-determinant range-separated LR theory [30] using a FCI long-range interacting wave function. Extrapolations have been obtained by finite differences with $\Delta\mu = 0.005a_0^{-1}$.

## 5. Results and discussion

### 5.1. Weight dependence of the ensemble and auxiliary energies

The two-state $^1\Sigma^+$ WIDFA range-separated ensemble energy and its extrapolation (see Equation (64)) have been computed for the stretched $HeH^+$ molecule when varying the ensemble weight $w$ for $\mu = 0.4$ and $\mu = 1$. Results are shown in Figure 2. Note that $2^1\Sigma^+$ is a charge-transfer state. LIM and ELIM ensemble energies are also plotted. By construction, both are linear in $w$, whereas the WIDFA ensemble energy is curved [22]. When $\mu = 0.4$, the curvature is significantly reduced by the extrapolation. In addition, the extrapolated WIDFA ensemble energy is much closer to FCI. Note also that the slope at $w = 0$, which corresponds to the auxiliary excitation energy associated with the ground-state density [22], becomes very close to the FCI one after extrapolation. This illustrates graphically the relevance of using extrapolated auxiliary energies for computing physical excitation energies [24,25]. For $\mu = 1.0$, the extrapolation has less impact simply because the WIDFA ensemble energy has a less pronounced curvature. The contribution of the srLDA functional to the energy is simply reduced. ELIM and extrapolated WIDFA ensemble energies are almost indistinguishable. This was expected since both WIDFA and LIM ensemble energies (with or without extrapolation) become equal to the (linear) FCI ensemble energy when $\mu \to +\infty$. Note, however, that for $\mu = 1.0$, the extrapolation enlarges the deviation of the ensemble
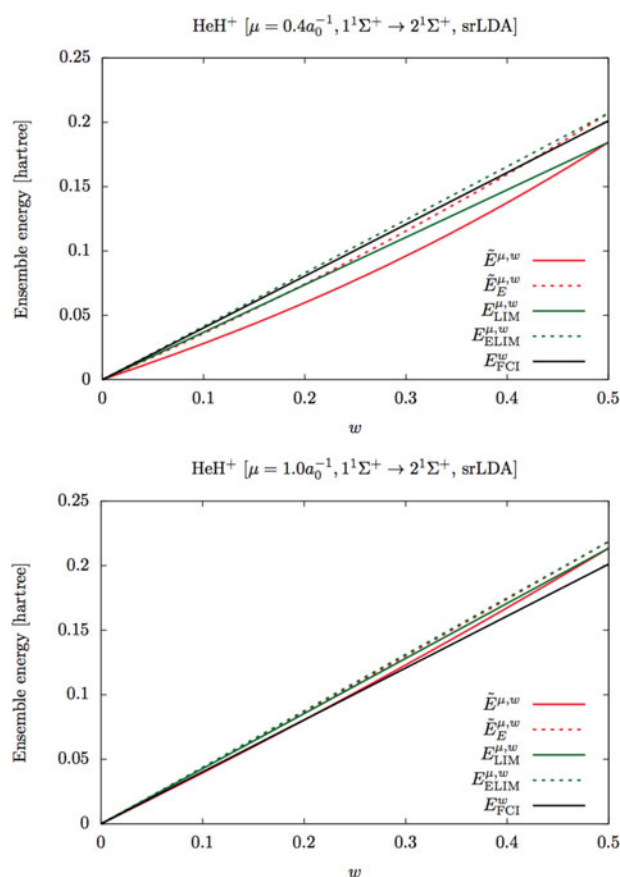


**Figure 2.** WIDFA and LIM ensemble energies computed with and without extrapolation for the stretched $HeH^+$ molecule at $\mu = 0.4$ (top panel) and $\mu = 1.0$ (bottom panel), when varying the ensemble weight $w$. Energies at $w = 0$ have been subtracted for ease of comparison. See text for further details.

energy from the FCI one. This will be analysed further in Section 5.2.

Let us now focus on the auxiliary excitation energies. In a previous work [22], some of the authors pointed out that the latter can be strongly weight-dependent, thus motivating the formulation of LIM. Extrapolation schemes are usually applied to auxiliary excitation energies based on the ground-state density [24,25]. In this section, we extrapolated from weight-dependent auxiliary excitation energies (see Equation (65)) for analysis purposes. Results are presented in Figure 3 for He, Be, and $HeH^+$, and in Figure 4 for $H_2$ in equilibrium and stretched geometries. As expected [22], the weight dependence of the auxiliary excitation energy before extrapolation is reduced when increasing $\mu$ from 0.4 to 1.0. For $\mu = 0.4$ and 1.0, the extrapolation reduces the weight dependence but, in general, it does not remove it completely.

### 5.2. Extrapolated LIM excitation energies

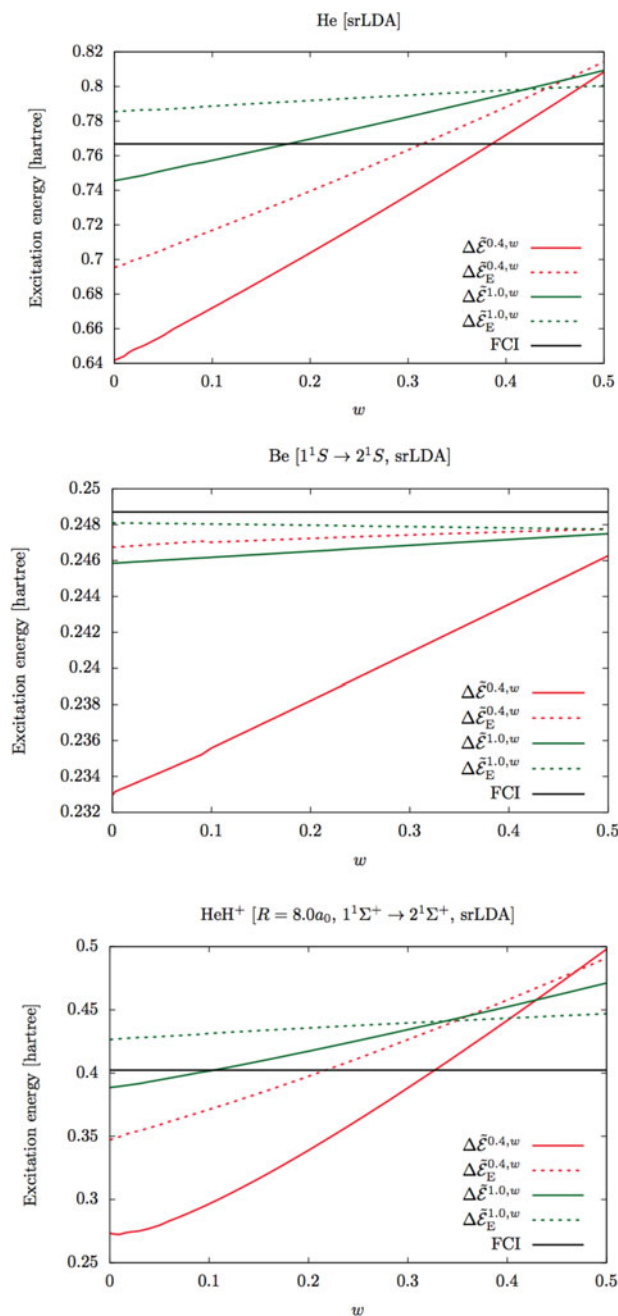As discussed previously, LIM provides approximate excitation energies which are weight-independent by

**Figure 3.** Auxiliary excitation energies computed with and without extrapolation for He (top panel), Be (middle panel), and the streched HeH$^+$ molecule (bottom panel) at $\mu = 0.4$ and $\mu = 1.0$, when varying the ensemble weight $w$. Comparison is made with FCI. See text for further details.



**Figure 4.** First auxiliary excitation energy computed with and without extrapolation for H$_2$ at equilibrium (top panel) and stretched (bottom panel) geometries with $\mu = 0.4$ and $\mu = 1.0$, when varying the ensemble weight $w$. Comparison is made with FCI. See text for further details.

construction. In this section, we investigate the impact of the extrapolation on the LIM excitation energies when varying $\mu$. For analysis purposes, comparison is made with the extrapolated auxiliary excitation energies based on the ground-state density. Results are presented in Figures 5 and 6.

Note that, by definition, the extrapolation has no effect at $\mu = 0$. On the other hand, with or without extrapolation, FCI excitation energies are recovered
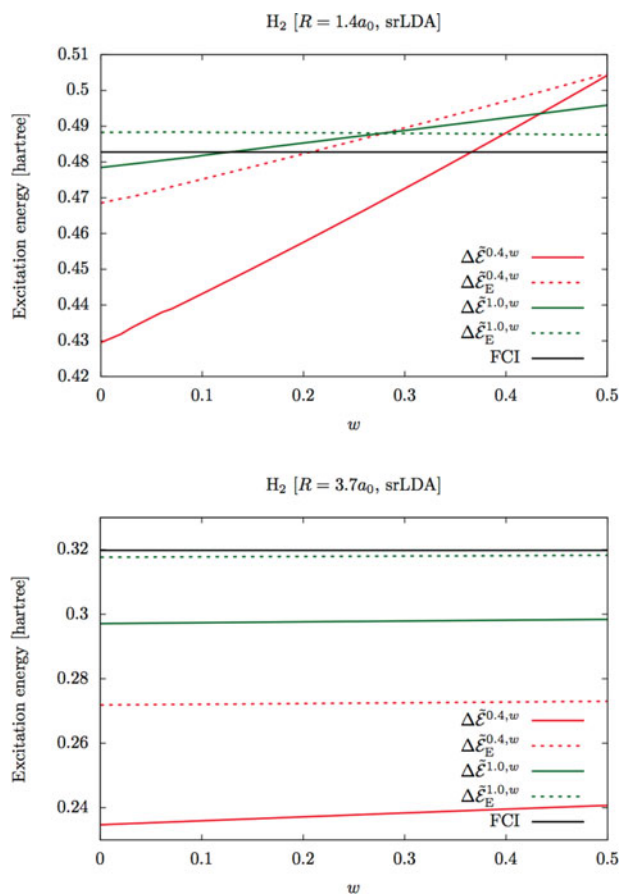
when $\mu \to +\infty$. Without extrapolation, LIM and auxiliary excitation energies are close to the FCI results when $\mu \geq 2.0$ for Be and H$_2$ at equilibrium (middle and bottom panels of Figures 5 and 6, respectively), and when $\mu \geq 3.0$ for He, HeH$^+$, and stretched H$_2$ (top and bottom panels of Figure 5 and bottom panel of Figure 6, respectively). We see that the extrapolation improves the convergence in $\mu$ of both LIM and auxiliary excitation energies towards the FCI values. However, better results are not systematically obtained for all $\mu$ values. In He, HeH$^+$, and H$_2$ at equilibrium, for example, the extrapolation makes LIM deviate from FCI when $0.5 \leq \mu \leq 1.0$. As shown in [25], this is related to the non-monotonic convergence of the excitation energies to the FCI values. Such a deterioration of LIM is also observed when $\mu$ is close to zero. The excitation energies are underestimated in that region and decrease with $\mu$. This pattern was not observed for the auxiliary excitation energies in [24,25], probably because the authors computed accurate short-range potentials along the range-separated adiabatic connection. It would be interesting, for
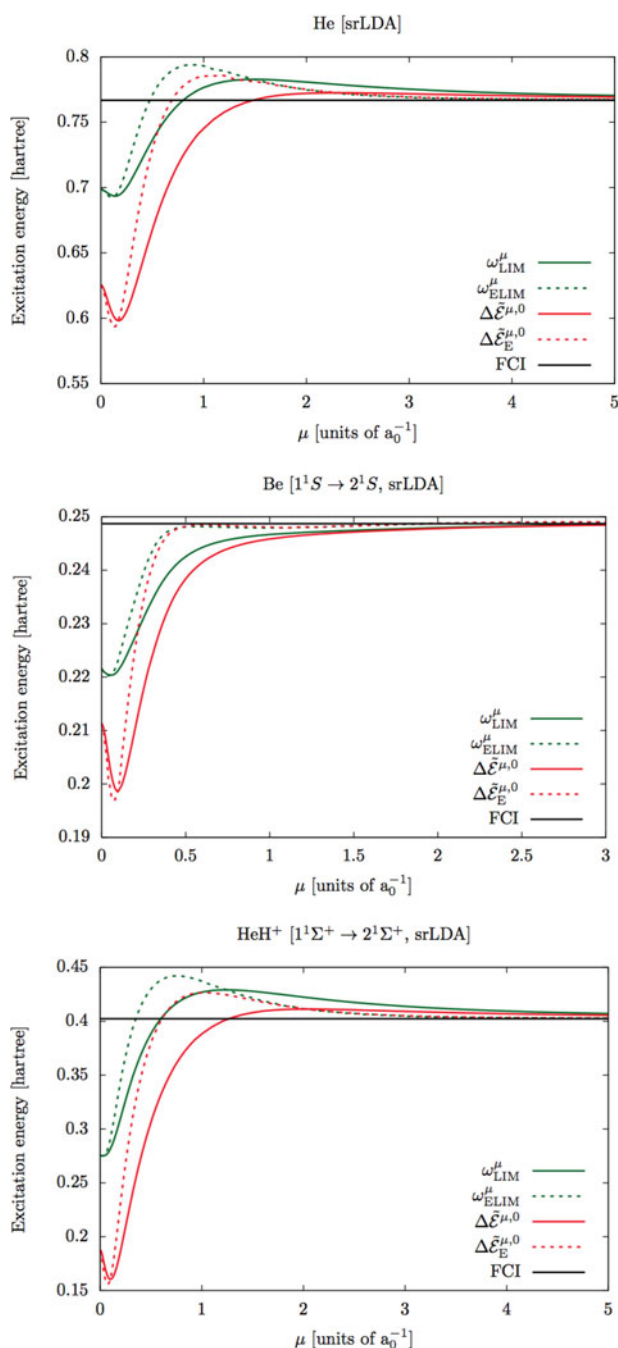
**Figure 5.** LIM excitation energies computed with and without extrapolation for He (top panel), Be (middle panel), and the stretched HeH$^+$ molecule (bottom panel), when varying $\mu$. Comparison is made with the auxiliary excitation energies and FCI.



**Figure 6.** First $^1\Sigma_g^+$ LIM excitation energy computed with and without extrapolation for H$_2$ at equilibrium (top panel) and stretched (bottom panel) geometries when varying $\mu$. Comparison is made with the auxiliary excitation energy and FCI.

### 5.3. $2^1\Sigma_g^+$ and $3^1\Sigma_g^+$ excitation energies in H$_2$

$2^1\Sigma_g^+$ and $3^1\Sigma_g^+$ excitation energies in H$_2$ have been computed along the bond-breaking coordinate with various methods. The range-separation parameter $\mu$ was set to the typical $\mu = 0.4$ value [34]. Results are presented in Figure 7. For analysis purposes, auxiliary excitation energies associated with the ground-state density ($w_0 = 0$) are compared with FCI and time-dependent multi-determinant range-separated LR results (see the top panel). In the equilibrium region ($R \approx 1.4a_0$), LR excitation energies are a bit closer to FCI values than the auxiliary excitation energies. This is due to the short-range kernel [22,30]. For larger bond distances ($3a_0 \leq R \leq 3.5a_0$), the avoided crossing obtained at the FCI level is not well reproduced. Auxiliary energies give almost a crossing while LR slightly increases the gap between the two excitation energies once again because of the short-range kernel. When approaching the dissociation limit, the latter does not contribute anymore to the $2^1\Sigma_g^+$ LR excitation energy that becomes identical to the auxiliary one. This is due to the doubly excited character of the

rationalisation purposes, to compare exact and srLDA LIM excitation energy expansions for small $\mu$ values. This is however, outside the scope of the current work.

Note finally that, for the typical $\mu = 0.4$ value [34], ELIM gives relatively accurate results. In the particular case of the stretched H$_2$ molecule, the improvement of the doubly excited $2^1\Sigma_g^+$ excitation energy after extrapolation is remarkable.
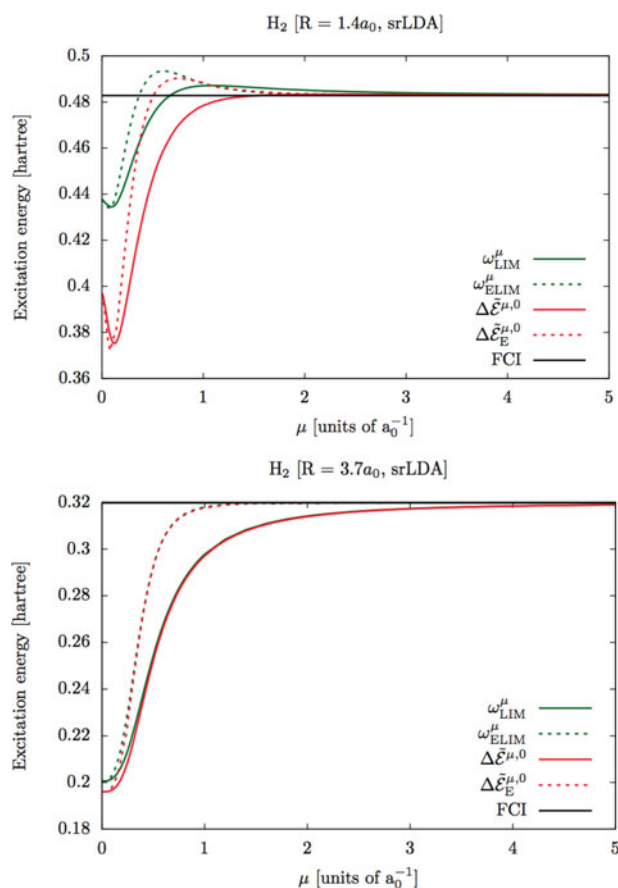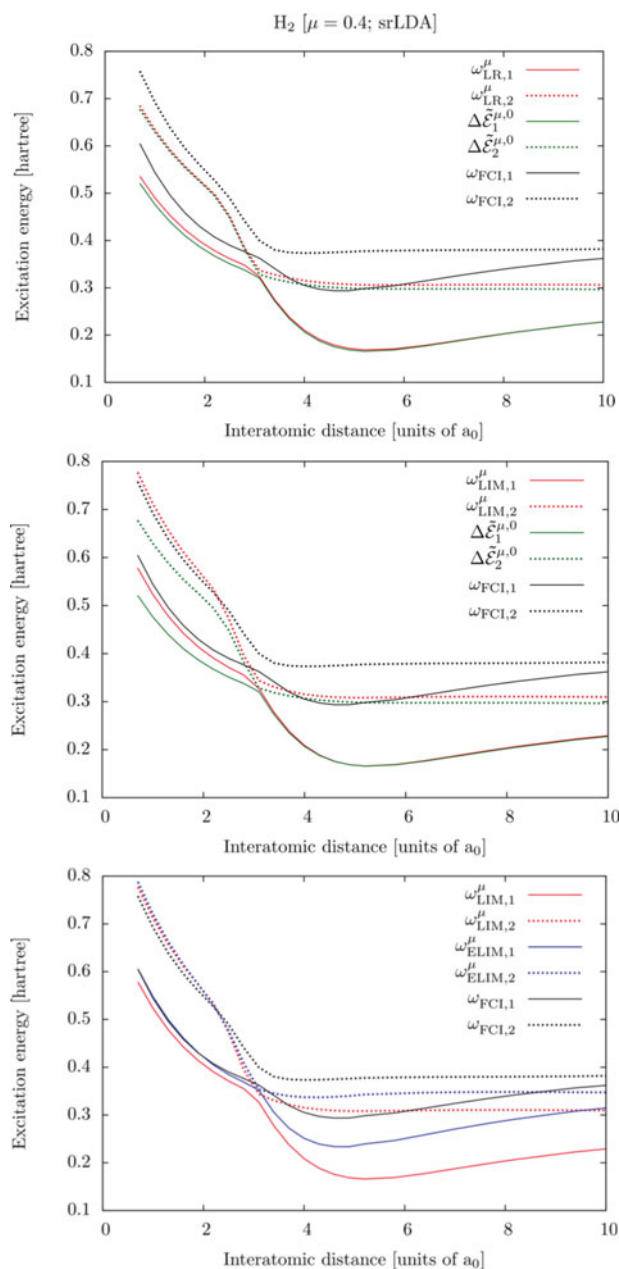
**Figure 7.** First and second $^1\Sigma_g^+$ excitation energies computed in $H_2$ along the bond-breaking coordinate with $\mu = 0.4$. Top panel: linear response (LR) versus auxiliary energies. Middle panel: LIM versus auxiliary energies. Bottom panel: LIM versus ELIM. Comparison is made with FCI. See text for further details.

excitation which does not induce changes in the density through first order [22,30]. Note the slight difference between $3^1\Sigma_g^+$ auxiliary and LR excitation energies. In this case, the short-range kernel does contribute. Let us finally point out that both range-separated approaches underestimate the excitation energies.

Let us now discuss the performance of LIM (middle panel of Figure 7). It is remarkable that, in the equilibrium region, LIM excitation energies are much more accurate than the auxiliary ones for both $2^1\Sigma_g^+$ and $3^1\Sigma_g^+$ states.

The avoided crossing is relatively well located within LIM but, like that at the LR level, it is not well reproduced (the states are too close in energy). For larger bond distances, $2^1\Sigma_g^+$ LIM and auxiliary excitation energies become identical, as expected [22]. On the other hand, those differ slightly for the $3^1\Sigma_g^+$ state. In summary, LIM significantly improves on both LR and auxiliary excitation energies only in the equilibrium region.

Turning to ELIM results (bottom panel of Figure 7), we first notice that, in the equilibrium region, the $2^1\Sigma_g^+$ excitation energy curve is almost on the top of the FCI one, as expected from the top panel of Figure 6. The extrapolation has less impact on the $3^1\Sigma_g^+$ state. For the latter, it actually enlarges the deviation from FCI. This is simply due to the fact that, without extrapolation, LIM already overestimates the $3^1\Sigma_g^+$ excitation energy. The positive slope in $\mu$ of the LIM excitation energy in the vicinity of $\mu = 0.4$, exactly like that for the $2^1\Sigma_g^+$ state (see the top panel in Figure 6), increases further the excitation energy. When the bond is stretched, ELIM improves on both individual excitation energies (both become much closer to the reference FCI values). The effect of the extrapolation becomes significant when approaching the dissociation limit. However, even though the avoided crossing remains relatively well located within ELIM, the two states become closer in energy after extrapolation. This shows how challenging it is to develop a reliable multi-determinant state-averaged range-separated DFT for modelling (avoided) crossings. It is still unclear if a ghost-interaction correction would provide better results. Work is currently in progress in this direction.

## 6. Perspective: a remedy for the ghost-interaction error in multi-determinant range-separated DFT

Unlike in Hartree–Fock theory, the exact cancellation of Hartree and exchange terms, for one electron systems, is not possible in KS-DFT when using local or semi-local functionals, thus inducing the so-called self-interaction errors. However, the use of orbital-dependent functionals can correct for this. Another type of error, referred to as ghost-interaction error [31], is introduced in ensemble DFT calculations when an ensemble density is inserted into the usual (or short-range) Hartree density functional. The ghost-interaction terms contain products of densities associated with different states. The use of local or semi-local exchange–correlation functionals cannot be expected to correct for such errors [17]. Note that, in multi-determinant range-separated ensemble DFT, densities are calculated from multi-determinant wave functions so that standard ghost-interaction

correction schemes, which have been developed in the context of GOK-DFT, cannot be used straightforwardly.

In the present section, we propose an alternative decomposition of the short-range ensemble exchange–correlation energy which has the advantage of being ghost-interaction-free. For that purpose, we use the concept of multi-determinantal (md) short-range exact exchange introduced by Toulouse et al. [41] in the context of ground-state range-separated DFT and extend it to ensembles as follows:

$$E_{\text{Hxc}}^{\text{sr},\mu,\mathbf{w}}[n] = E_{\text{H}}^{\text{sr},\mu}[n] + E_{\text{x,md}}^{\text{sr},\mu,\mathbf{w}}[n] + E_{\text{c,md}}^{\text{sr},\mu,\mathbf{w}}[n], \quad (69)$$

where

$$E_{\text{x,md}}^{\text{sr},\mu,\mathbf{w}}[n] = \text{Tr}\left[\hat{\Gamma}^{\mu,\mathbf{w}}[n]\hat{W}_{\text{ee}}^{\text{sr},\mu}\right] - E_{\text{H}}^{\text{sr},\mu}[n], \quad (70)$$

and, according to Equations (33) and (34),

$$E_{\text{c,md}}^{\text{sr},\mu,\mathbf{w}}[n] = E_{\text{c}}^{\text{sr},\mu,\mathbf{w}}[n] + \text{Tr}\left[\hat{\Gamma}_{s}^{\mathbf{w}}[n]\hat{W}_{\text{ee}}^{\text{sr},\mu}\right]$$
$$- \text{Tr}\left[\hat{\Gamma}^{\mu,\mathbf{w}}[n]\hat{W}_{\text{ee}}^{\text{sr},\mu}\right]. \quad (71)$$

Note that the expression in Equation (70) involves the ensemble density matrix of the long-range interacting system with ensemble density $n$ rather than the noninteracting one (see Equation (34) for comparison). Finally, the complementary short-range correlation functional $E_{\text{c,md}}^{\text{sr},\mu}[n]$ that is adapted to the exact multi-determinant short-range exchange of Toulouse et al. [41] is recovered in the ground-state limit ($w_0 = 1$). Since, according to Equation (37),

$$\hat{\Gamma}^{\mu,\mathbf{w}}[n_{\hat{\Gamma}^{\mu,\mathbf{w}}}] = \hat{\Gamma}^{\mu,\mathbf{w}}, \quad (72)$$

combining the alternative decomposition in Equation (69) with Equation (36) leads to the exact ensemble energy expression as follows:

$$E^{\mathbf{w}} = \text{Tr}\left[\hat{\Gamma}^{\mu,\mathbf{w}}\left(\hat{T} + \hat{W}_{\text{ee}} + \hat{V}_{\text{ne}}\right)\right] + E_{\text{c,md}}^{\text{sr},\mu,\mathbf{w}}[n_{\hat{\Gamma}^{\mu,\mathbf{w}}}]. \quad (73)$$

Like in the ground-state theory, this expression *cannot* be variational with respect to the ensemble density matrix, otherwise double-counting problems would occur [29]. Optimised effective potential techniques should be applied in this context to avoid such problems [29]. A simple approximation would consist in replacing the exact auxiliary ensemble density matrix with the one obtained at the WIDFA level (see Equation (47)):

$$\hat{\Gamma}^{\mu,\mathbf{w}} \to \hat{\gamma}^{\mu,\mathbf{w}}. \quad (74)$$

Moreover, in the spirit of WIDFA, one could use the ground-state correlation functional, for which a LDA has been developed [42], rather than the ensemble functional (for which no approximations have been developed so far):

$$E_{\text{c,md}}^{\text{sr},\mu,\mathbf{w}}[n] \to E_{\text{c,md}}^{\text{sr},\mu}[n]. \quad (75)$$

Note that the resulting approximate ensemble energy will be ghost-interaction-free. Interestingly, the alternative separation of short-range ensemble exchange and correlation energies is a way to introduce (implicitly) weight dependence into the short-range ensemble functional. The resulting approximate ensemble energy may also have less curvature in the ensemble weights than the WIDFA one, but to ensure this would require numerical investigation. Note finally that LIM can also be applied in this context in order to compute excitation energies.

## 7. Conclusion

The extrapolation scheme initially proposed by Savin [23] in the context of ground-state range-separated DFT has been extended to ensembles of ground and excited states. This can be achieved when expanding the range-separated ensemble energy in powers of $1/\mu$, where $\mu$ is the parameter that controls the range separation of the two-electron repulsion. Combining this approach with the recently proposed LIM [22] enables to compute excitation energies that, by construction, do not depend on the choice of the ensemble weights. We have shown on a small test set consisting of He, Be, $H_2$, and $HeH^+$ that, for the typical $\mu = 0.4$ value, the ELIM can provide accurate (sometimes very accurate) excitation energies even for charge-transfer and doubly excited states. It was also shown that, in the stretched $H_2$ molecule, the extrapolation can improve on excitation energies individually but the relative excitation energy can be deteriorated, thus leading to an inaccurate description of avoided crossings. Such problems should be investigated further in the future in order to turn multi-determinant range-separated DFT into a reliable computational tool for modelling photochemistry, for example. A potential source of errors in LIM and ELIM calculations is the so-called ghost-interaction error that is introduced when inserting an ensemble density into the short-range Hartree functional. We proposed an alternative separation of ensemble short-range exchange and correlation energies which, in principle, enables the calculation of ghost-interaction-free excitation energies in the context of multi-determinant range-separated ensemble DFT. Work is currently in progress in this direction.

## Acknowledgments

The authors are pleased to dedicate this work to Andreas Savin on the occasion of his 65th birthday (congratulations Andreas and thanks for everything !). E. Fromager would like to thank Julien Toulouse for stimulating discussions on extrapolation schemes. E.D. Hedegård acknowledges the Villum Kann Rasmussen foundation for a post-doc fellowship.

## Disclosure statement

No potential conflict of interest was reported by the authors.

## Funding

E. Fromager acknowledges financial support from the LABEX 'Chemistry of complex systems' and the ANR (MCFUNEX project).

## References

[1] M. Marques and E. Gross, Annu. Rev. Phys. Chem. **55**, 427 (2004).
[2] M. Casida and M. Huix-Rotllant, Annu. Rev. Phys. Chem. **63**, 287 (2012).
[3] N.T. Maitra, F. Zhang, R.J. Cave, and K. Burke, J. Chem. Phys. **120**, 5932 (2004).
[4] O. Gritsenko, S. Van Gisbergen, A. Gorling, and E. Baerends, J. Chem. Phys. **113**, 8478 (2000).
[5] A.K. Theophilou, J. Phys. C **12**, 5419 (1979).
[6] E.K.U. Gross, L.N. Oliveira, and W. Kohn, Phys. Rev. A **37**, 2805 (1988).
[7] E.K.U. Gross, L.N. Oliveira, and W. Kohn, Phys. Rev. A **37**, 2809 (1988).
[8] E.K.U. Gross, L.N. Oliveira, and W. Kohn, Phys. Rev. A **37**, 2821 (1988).
[9] A. Nagy, J. Phys. B: At. Mol. Opt. Phys. **29**, 389 (1996).
[10] G. Paragi, I. Gyémánt, and V.V. Doren, Chem. Phys. Lett. **324**, 440 (2000).
[11] G. Paragi, I. Gyémánt, and V.V. Doren, J. Mol. Struct. (Theochem) **571**, 153 (2001).
[12] K. Pernal, N.I. Gidopoulos, and E. Pastorczak, Adv. Quantum Chem. (2015).
[13] O. Franck and E. Fromager, Mol. Phys. **112**, 1684 (2014).
[14] A. Pribram-Jones, Z. hui Yang, J.R.Trail, K. Burke, R.J. Needs, and C. A. Ullrich, J. Chem. Phys. **140**, 18A541 (2014).
[15] Z.h. Yang, J.R. Trail, A. Pribram-Jones, K. Burke, R.J. Needs, and C.A. Ullrich, Phys. Rev. A **90**, 042501 (2014).
[16] A. Nikiforov, J.A. Gamez, W. Thiel, M. Huix-Rotllant, and M. Filatov, J. Chem. Phys. **141**, 124122 (2014).
[17] E. Pastorczak and K. Pernal, J. Chem. Phys. **140**, 18A514 (2014).
[18] M. Filatov, M. Huix-Rotllant, and I. Burghardt, J. Chem. Phys. **142**, 184104 (2015).
[19] M. Filatov, WIREs Comput. Mol. Sci. **5**, 146 (2015).
[20] A. Savin, *Recent Developments and Applications of Modern Density Functional Theory* (Elsevier, Amsterdam, 1996), p. 327.
[21] E. Pastorczak, N.I. Gidopoulos, and K. Pernal, Phys. Rev. A **87**, 062501 (2013).
[22] B. Senjean, S. Knecht, H.J.Aa. Jensen, and E. Fromager, Phys. Rev. A **92**, 012518 (2015).
[23] A. Savin, J. Chem. Phys. **140**, 18A509 (2014).
[24] E. Rebolini, J. Toulouse, A.M. Teale, T. Helgaker, and A. Savin, J. Chem. Phys. **141**(4), 044123 (2014).
[25] E. Rebolini, J. Toulouse, A.M. Teale, T. Helgaker, and A. Savin, Phys. Rev. A **91**, 032519 (2015).
[26] P. Hohenberg and W. Kohn, Phys. Rev. **136**, B864 (1964).
[27] W. Kohn and L. Sham, Phys. Rev. **140**, A1133 (1965).
[28] J. Toulouse, F. Colonna, and A. Savin, Phys. Rev. A **70**, 062505 (2004).
[29] A. Stoyanova, A.M. Teale, J. Toulouse, T. Helgaker, and E. Fromager, J. Chem. Phys. **139**, 134113 (2013).
[30] E. Fromager, S. Knecht, and H.J. Aa. Jensen, J. Chem. Phys. **138**, 084101 (2013).
[31] N. Gidopoulos, P. Papaconstantinou, and E. Gross, Phys. Rev. Lett. **88**, 033003 (2002).
[32] A. Nagy, Int. J. Quantum Chem. **69**, 247 (1998).
[33] P. Gori-Giorgi and A. Savin, Phys. Rev. A **73**, 032506 (2006).
[34] E. Fromager, J. Toulouse, and H.J.Aa. Jensen, J. Chem. Phys. **126**, 74111 (2007).
[35] K. Aidas, C. Angeli, K.L. Bak, V. Bakken, R. Bast, L. Boman, O. Christiansen, R. Cimiraglia, S. Coriani, P. Dahle, E.K. Dalskov, U. Ekström, T. Enevoldsen, J.J. Eriksen, P. Ettenhuber, B. Fernández, L. Ferrighi, H. Fliegl, L. Frediani, K. Hald, A. Halkier, C. Hättig, H. Heiberg, T. Helgaker, A.C. Hennum, H. Hettema, E. Hjertenæs, S. Høst, I.M. Høyvik, M.F. Iozzi, B. Jansík, H.J.Aa. Jensen, D. Jonsson, P. Jørgensen, J. Kauczor, S. Kirpekar, T. Kjærgaard, W. Klopper, S. Knecht, R. Kobayashi, H. Koch, J. Kongsted, A. Krapp, K. Kristensen, A. Ligabue, O.B. Lutnæs, J.I. Melo, K.V. Mikkelsen, R.H. Myhre, C. Neiss, C.B. Nielsen, P. Norman, J. Olsen, J.M.H. Olsen, A. Osted, M.J. Packer, F. Pawlowski, T.B. Pedersen, P.F. Provasi, S. Reine, Z. Rinkevicius, T.A. Ruden, K. Ruud, V.V. Rybkin, P. Sałek, C.C.M. Samson, A.S. de Merás, T. Saue, S.P.A. Sauer, B. Schimmelpfennig, K. Sneskov, A.H. Steindal, K.O. Sylvester-Hvid, P.R. Taylor, A.M. Teale, E.I. Tellgren, D.P. Tew, A.J. Thorvaldsen, L. Thøgersen, O. Vahtras, M.A. Watson, D.J.D. Wilson, M. Ziolkowski, and H. Ågren, WIREs Comput. Mol. Sci. **4**, 269 (2015).
[36] DALTON, a molecular electronic structure program, Release Dalton2015 (2015). http://daltonprogram.org/.
[37] J. Toulouse, A. Savin, and H.J. Flad, Int. J. Quantum Chem. **100**, 1047 (2004).
[38] E. Goll, H.J. Werner, and H. Stoll, Phys. Chem. Chem. Phys. **7**, 3917 (2005).
[39] T.H. Dunning, Jr, J. Chem. Phys. **90**, 1007 (1989).
[40] D.E. Woon and T.H. Dunning, Jr, J. Chem. Phys. **100**, 2975 (1994).
[41] J. Toulouse, P. Gori-Giorgi, and A. Savin, Theor. Chem. Acc. **114**, 305 (2005).
[42] S. Paziani, S. Moroni, P. Gori-Giorgi, and G.B. Bachelet, Phys. Rev. B **73**, 155111 (2006).